Bathyal benthic megafauna from the Mid-Atlantic Ridge in the region of the Charlie-Gibbs fracture zone based on remotely operated vehicle observations

Claudia H.S. Alt[a,b], Antonina Kremenetskaia (Rogacheva)[c], Andrey V. Gebruk[c], Andrew J. Gooday[a], Daniel O.B. Jones[a,*]

[a] National Oceanography Centre, University of Southampton Waterfront Campus, European Way, Southampton SO14 3ZH, United Kingdom
[b] University of Southampton, University Road, Southampton SO17 1BJ, United Kingdom
[c] P.P. Shirshov Institute of Oceanology, Russian Academy of Sciences, Nakhimovsky Pr., 36, 117997 Moscow, Russia

ARTICLE INFO

ABSTRACT

Mid-ocean ridges are important geological features that cover around 33% of the global ocean floor, increase environmental heterogeneity on a regional scale and influence benthic community ecology. Benthic communities at the Mid-Atlantic Ridge (MAR) were studied at four contrasting sites, located east and west of the ridge, which were further separated into northern (54°N) and southern (48°N) sites by the Charlie-Gibbs Fracture Zone (CGFZ) and the Sub-Polar Front (SPF). The MAR in the CCFZ region area had flat areas surrounded by gentle slopes between rocky cliffs. A total of 32 remotely operated vehicle video transects (32,000 m² of seafloor) were surveyed on the flat areas and sedimented slopes (10°). In total, 154 distinct taxonomic units were identified (from 9 phyla) across all sites. The sediments of the flat and sloping sites were generally similar, but differences were seen in the community composition and faunal abundance (~ 4 times higher in the flat sites, except at the northwestern site). Significant differences in abundance were observed between sites (highest in the northern sites). The two northern sites had distinct community compositions, while the two southern sites were similar. This suggests that the MAR acts as a stronger barrier between communities north of the CGFZ than it does to the south. There was high heterogeneity between transects and it was not possible to identify general drivers for the benthic megafauna at the MAR. Our results emphasize the limited knowledge of this vast system with its unique benthic megafauna.

1. Introduction

In terrestrial environments the ecological importance of barriers to dispersal is well recognised (e.g. MacArthur and Wilson, 1967). In the oceans, in contrast, little is known in detail about the effects of such barriers, which may include topographic features, such as mid-ocean ridges, or isolating hydrography. Mid-ocean ridges are one of the most prominent landforms on earth. They cover around 33% of the global ocean floor, providing a large bathyal habitat flanked by abyssal plains, distant from the continental margins, and hosting an enhanced benthic biomass (Priede et al., 2013a). The processes controlling the diversity and connectivity of benthic communities within ridge systems and between ridges and adjacent margins are poorly understood. Most of our knowledge of these key processes comes from areas in the vicinity of land masses and far away from mid-ocean ridges, where oceanographic properties and dynamics (Christiansen and Thiel, 1992; Woodgate and Fahrbach, 1999), food supply (Lampitt, 1985) and habitat type (Rex, 1981; Auster et al., 1991) are thought to play a key role in controlling the distribution, density and diversity of fauna.

Large submarine features such as mid-ocean ridges greatly increase environmental heterogeneity on a regional scale, leading to more complex and diverse communities (Levin et al., 2001). Habitat heterogeneity and complexity can be modified across a wide range of scales by abiotic processes, for example, plate tectonics, hydrography (from thermohaline circulation to wind/tide-driven hydrography; Thistle et al., 1991), and sediment supply and transport (Snelgrove and Smith, 2002). Biotic processes that manipulate the sediment are also important and affect habitat heterogeneity at regional to very fine (centimetre) scales. Most studies focus on local-scale processes that increase habitat heterogeneity, such as spatiotemporal variation in

resource availability (Lampitt et al., 1995), disturbance (McClain and Barry, 2010), bioturbation (Bell et al., 2013), formation of biogenic structures (Buhl-Mortensen et al., 2010; Beaulieu, 2001; Hughes and Gooday, 2004), sediment properties (Rex, 1981) and local-scale oceanography and hydrodynamics (McClain and Barry, 2010; Wildish and Kristmanson, 1997). However, multiple interacting factors often make it difficult to interpret complex patterns and to discern the controls on benthic community ecology.

Imaging techniques are commonly used to assess habitats and associated faunal patterns (Grassle, 1991). Images and videos have become very important for understanding deep-sea habitats as they can be obtained using non-destructive methods that reveal concurrent information on habitat heterogeneity and species-habitat interactions (Bell et al., 2016). They also provide insights into community attributes such as diversity and densities (Simon-Lledó et al., 2019), as well as behaviours including predation and other forms of feeding (Lebrato and Jones, 2009), locomotion, burrowing, and intra-specific interactions, e.g. pairing (Tyler et al., 1992), as well as inter-specific interactions (Gooday et al., 2013; Shields et al., 2013). Long-term monitoring studies have likewise benefited from camera systems that reveal community changes (Glover et al., 2010) linked to the quality of phytodetritus reaching the sea floor in the Atlantic (Morris et al., 2016) and the Pacific (Kuhnz, 2014). Finally, the effects of large-scale natural (Staudigel et al., 2006) and anthropogenic (Jones et al., 2012) disturbances can be quantified and monitored using visual tools (Glover et al., 2010).

Although the Mid-Atlantic Ridge (MAR) is one of the better-studied mid-ocean ridges, its biological significance is only beginning to be understood (Bergstad et al., 2008a; Vecchione et al., 2010; Priede et al., 2013b). In this paper we use high-resolution imagery to explore the diversity, density, distribution and community structures of epibenthic megafauna associated with the MAR in the vicinity of the Charlie-Gibbs Fracture Zone (CGFZ) and Sub-Polar Front (SPF). Four discrete sites were investigated in detail with the aim of assessing the influence on epibenthic megafauna of 1) the potential barrier provided by the ridge and associated fracture zone, and 2) the slope of the seafloor.

2. Methods

Samples were collected from the MAR at bathyal depths (~ 2500 m depth) as part of the ECOMAR project (Priede et al., 2013). Four stations were targeted: SE (48°58′N, 27°51′W), SW (48°44′N, 28°39′W), NE (54°05′N, 33°58′W), and NW (54°19′N, 36°01′W) of the CGFZ (Fig. 1). Video transects were obtained during RRS James Cook cruise JC048 (26 May – 3 July 2010) with the UK National Marine Facilities Remotely Operated Vehicle (ROV) Isis. The ROV was equipped with two high-definition (HD) colour video cameras (Insite Mini Zeus), a 3-chip colour standard-definition video (Insite Pegasus), digital still camera (Insite Scorpio) and Hydrargyrum medium-arc iodide (HMI) lighting. A set of two parallel lasers (100 mm apart) was mounted on each HD camera for scaling. One HD camera was mounted vertically on the tool tray with a HMI light mounted at an angle to illuminate the field of view (1.5 m separation). Only the vertical camera was used for quantitative ecological assessment. The other HD camera was mounted on a pan-and-tilt unit at the front of the ROV. This was used to take zoomed-in, oblique video images to help with species identifications.

The ROV was equipped with both ultra-short baseline navigation (Sonardyne medium frequency USBL) to provide absolute global position (accuracy approximately ± 10 m), and Doppler velocity log navigation (RDI DVL 1200 kHz) to provide very accurate relative position (± 0.1 m). During every transect the ROV was run in a straight line, on a set bearing, at a constant speed (0.13 ms) and at the same set altitude (2 m). The ROV was flown while maintaining Doppler lock on the seafloor, enabling very precise control. Transect width (2 m; max variation ± 0.1 m) was maintained over an uneven seafloor by adjusting ROV altitude in 50 mm steps to ensure that parallel laser beams projected onto the seafloor (100 mm apart on the seafloor) were

constantly the same distance apart on the screen (5% of screen width). Over the 500 m long transect, this technique imaged 1000 m^2 of seafloor and 2000 m^3 of overlying suprabenthic water. HD video was recorded (AJA 71 KiPro) and stored as full resolution digital files on a hard drive (DroboPro).

2.1. Survey design

The geomorphology of this area of the MAR flank is characterised by flat terraces separated by linear elevations parallel to the ridge axis (Priede et al., 2013b). On the side facing away from the ridge axis there are gentle sedimented slopes and on the side facing the ridge axis there are steep rocky cliffs (Bell et al., 2016). This study aimed to assess the changes in megafaunal assemblages between the generally sedimented areas of the MAR: the flat terraces (0–2° slope) and the gentle slopes (typically around 10° slope), which are henceforth referred to as habitats. The megafauna of the steep rocky cliff areas has already been documented (Bell et al., 2016).

Bathymetry data were used to differentiate habitats. Bathymetry data were collected on the RRS James Cook ECOMAR cruise in 2007 (JC11) with a Kongsberg EM120 swath bathymetry system (Priede et al., 2013). Within each study site (~ 2500 m depth) two slope types (habitats) were investigated (Fig. 1): flat (the terraces with 0–2° slope) and 10° slope (8–12° slopes). The area of each habitat was delineated by polygons using ArcGIS (Version 10, ESRI). For each habitat in turn, polygons were selected (largest area first) until > 0.5 km^2 of seabed was covered; all remaining polygons were removed automatically. Within the selected polygons 100 lines were generated starting at random start points; the lines were 500 m long and with a 15° heading, along the ridge axis. All lines that intersected with polygon boundaries were removed. For each habitat, four non-overlapping lines were picked at random from the remaining lines. These four lines became the ROV sampling transects for each habitat at every site. The sampling unit for all analyses was a 500 m long ROV transect, resulting in a total of 32 sampling units (Table 1).

2.2. Video processing

Transect lengths were standardised to 500 m (covering 1000 m^2 of seabed) using smoothed Doppler velocity log data. For analysis, HD video was displayed using Quicktime Pro (version 7, Apple Inc.). Identifications and abundance counts were made to the closest possible taxonomic unit, using the HD video footage from the vertical camera. This resulted in a species abundance matrix, with all occurrences recorded against the time in the video where they appeared. To ensure quality, the identifications and occurrences noted were rechecked in still frames from each video transect. One still frame was extracted every second using Final Cut Pro (X 10.0 Apple Inc.), and given a unique ID code. The frames containing every record in the species abundance matrix were automatically extracted using a programme written in the R software environment (R Development Core Team, 2009). These were manually screened to check for consistency in identification and to validate counts. Once this was completed, taxonomic experts checked and confirmed species identities where necessary (see acknowledgments).

2.3. Analyses

Taxa included in analysis were strictly epibenthic fauna > 10 mm in size, including both sessile and motile species, and excluding swimming (e.g. fishes, which are reported in Linley et al., 2013, and crustaceans) and drifting taxa (e.g. gelatinous zooplankton). Also excluded were organisms that could not be identified to at least phylum level and those that could not be distinguished from traces with certainty. Observations that were excluded based on these criteria were quantified and comprised about 17% of the total count. Small
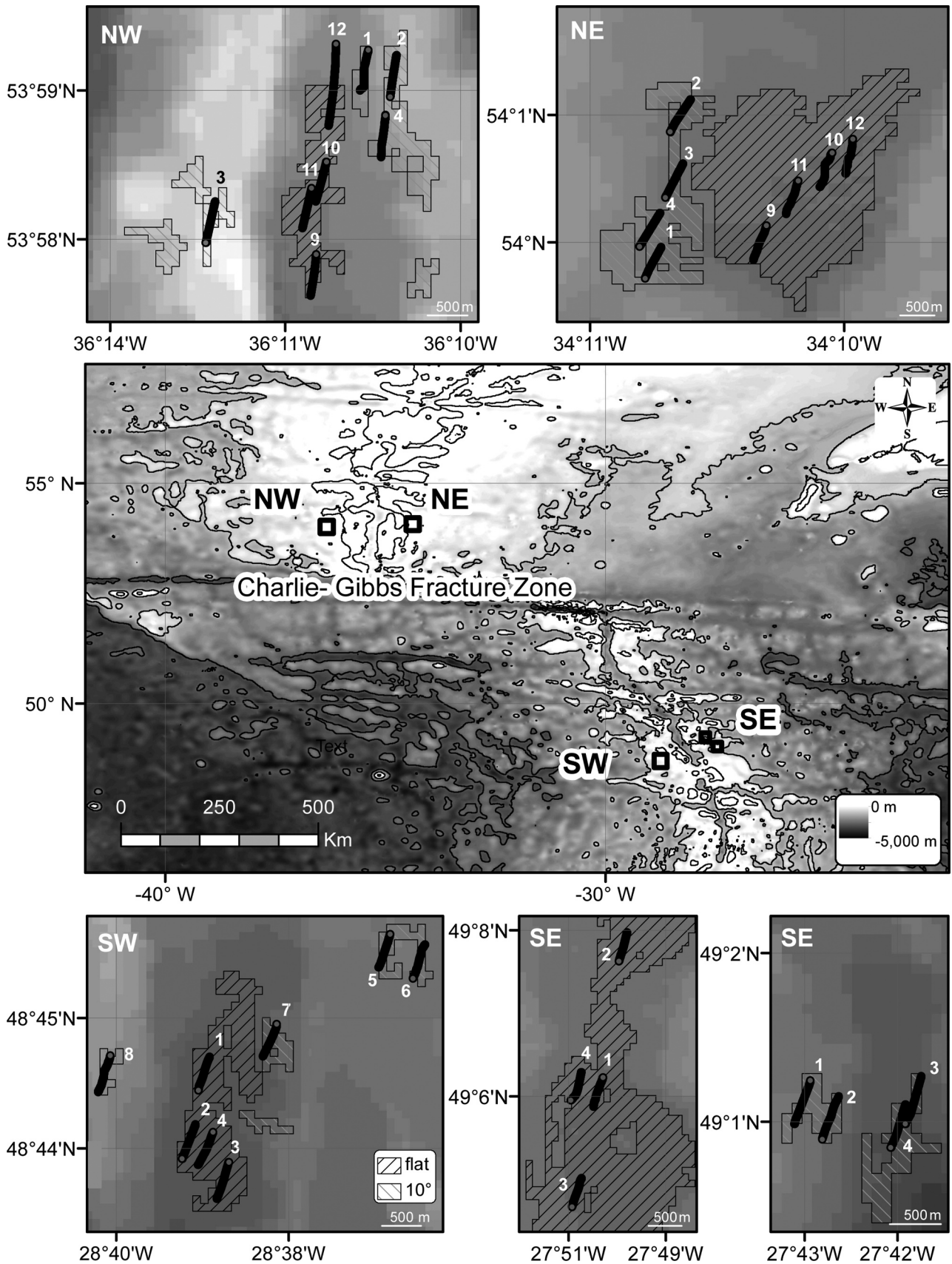
Fig. 1. Survey Map: The central map shows the general sample area around the Charlie-Gibbs Fracture Zone, highlighting the four sample sites and the bathymetry of the area. The individual sites are shown in their relative positions, indicating the habitat type and the individual transects that were analysed, together with the respective transect number (Table 1).

Table 1

Start and end points of straight-line ROV video transects. All positions are in Latitude and Longitude (degrees and decimal minutes). Datum is WGS1984. Date as day, month, year. Time as UTC/ GMT.

Name	Lat_start		Long_start		Lat_end		Long_end		Date and time of transect start	Average depth, m
	Deg.	Min.	Deg.	Min.	Deg.	Min.	Deg.	Min.		
NW1-10°	53	59.00	− 36	11.15	53	59.26	− 36	11.05	06/06/2010 02:33:30	2470
NW2-10°	53	58.97	− 36	10.82	53	59.23	− 36	10.73	06/06/2010 04:16:28	2400
NW3-10°	53	57.96	− 36	12.89	53	58.22	− 36	12.79	05/06/2010 14:13:59	2238
NW4-10°	53	58.56	− 36	10.91	53	58.82	− 36	10.81	06/06/2010 00:41:02	2452
NW9-flat	53	57.62	− 36	11.71	53	57.88	− 36	11.62	05/06/2010 18:40:17	2542
NW10-flat	53	58.25	− 36	11.64	53	58.52	− 36	11.54	05/06/2010 22:42:22	2533
NW11-flat	53	58.07	− 36	11.80	53	58.34	− 36	11.70	05/06/2010 21:05:27	2540
NW12-flat	53	58.77	− 36	11.50	53	59.31	− 36	11.42	01/06/2010 15:46:42	2507
NE1-10°	53	59.73	− 34	11.54	53	59.99	− 34	11.44	11/06/2010 19:31:35	2420
NE2-10°	54	0.86	− 34	11.33	54	1.12	− 34	11.21	11/06/2010 14:51:30	2445
NE3-10°	54	0.35	− 34	11.38	54	0.61	− 34	11.27	11/06/2010 16:35:40	2461
NE4-10°	53	59.98	− 34	11.57	54	0.23	− 34	11.46	11/06/2010 18:00:43	2420
NE9-flat	53	59.86	− 34	10.72	54	0.13	− 34	10.61	11/06/2010 06:25:15	2505
NE10-flat	54	0.43	− 34	10.21	54	0.70	− 34	10.10	11/06/2010 09:19:45	2501
NE11-flat	54	0.22	− 34	10.46	54	0.47	− 34	10.36	11/06/2010 07:56:16	2500
NE12-flat	54	0.55	− 34	9.98	54	0.80	− 34	9.86	11/06/2010 11:01:01	2502
SW1-flat	48	44.45	− 28	39.04	48	44.71	− 28	38.91	18/06/2010 18:59:04	2613
SW2-flat	48	43.91	− 28	39.20	48	44.17	− 28	39.07	16/06/2010 18:21:28	2630
SW3-flat	48	43.63	− 28	38.83	48	43.89	− 28	38.71	16/06/2010 14:48:10	2634
SW4-flat	48	43.87	− 28	39.02	48	44.12	− 28	38.90	16/06/2010 16:44:20	2628
SW5-10°	48	45.38	− 28	36.95	48	45.64	− 28	36.83	19/06/2010 04:17:01	2413
SW6-10°	48	45.30	− 28	36.55	48	45.56	− 28	36.42	19/06/2010 06:06:43	2439
SW7-10°	48	44.69	− 28	38.28	48	44.95	− 28	38.15	18/06/2010 23:17:00	2565
SW8-10°	48	44.45	− 28	40.19	48	44.71	− 28	40.06	18/06/2010 10:34:20	2306
SE1-flat	49	5.91	− 27	50.32	49	6.17	− 27	50.19	24/06/2010 00:51:14	2757
SE2-flat	49	7.23	− 27	49.99	49	7.48	− 27	49.86	23/06/2010 18:20:55	2739
SE3-flat	49	5.00	− 27	50.62	49	5.26	− 27	50.48	24/06/2010 05:27:35	2756
SE4-flat	49	5.96	− 27	50.62	49	6.22	− 27	50.49	23/06/2010 22:40:01	2749
SE1-10°	49	0.98	− 27	43.42	49	1.24	− 27	43.29	27/06/2010 03:02:15	2463
SE2-10°	49	0.90	− 27	43.16	49	1.15	− 27	43.03	27/06/2010 01:32:20	2500
SE3-10°	49	1.01	− 27	42.41	49	1.27	− 27	42.28	26/06/2010 21:55:18	2661
SE4-10°	49	0.85	− 27	42.55	49	1.11	− 27	42.41	26/06/2010 23:17:08	2633

gastropods and bivalves were also excluded because they could not be distinguished with certainty from the pteropod shells that carpeted the seafloor in some areas.

Of the species differentiated by morphology from the images, many could not be identified to species level. The level of taxonomic identification that was possible was highlighted in the names of the indeterminate ('indet.') taxa; for example, Holothurian (Class) indet. could only be identified to class level. Some taxa with similar morphologies could not be consistently distinguished and were grouped; for example, two echinoid species (belonging to two different orders) were referred to as Urechinidae/Hemiasteridae complex. All operational taxonomic units (OTU), regardless of their level of identification, were treated statistically as species (e.g., counts of Holothurian (Class) indet. were treated in the same way as *Staurocucumis abyssorum*). This approach has been successfully applied in other studies (Gutt and Piepenburg, 2003; Jones et al., 2007; Soltwedel et al., 2009).

Species richness in this study refers to the number of distinct OTUs for a given number of observations and was determined from species accumulation curves, created following Colwell et al. (2004) in R and checked against the output of the Estimate-S software.

Standing stock refers to the number of specimens in a given area (Grey, 2000). In the present study this means the number of individual specimens in 8000 m² area sampled when comparing sites, and 4000 m² when comparing habitats. In order to test for the effects of slope and site on standing stock, a generalised linear model (glm) was carried out in the R environment (R Development Core Team, 2009), with site, slope and the interaction set as factors and standing stock as the response variable. The residual deviance (32019) was greater than the residual degrees of freedom (24), indicating over-dispersion. The model was, therefore, fitted with quasi-Poisson errors using the R function glm and the ANOVA function of the R package CAR (companion to applied

regression) (Fox and Weisberg, 2011) in the R programming environment (R Development Core Team, 2009).

Multivariate analysis was used to assess changes in community structure in response to habitat and site. Prior to multivariate analysis the species abundances were square-root transformed, owing to the large numbers of species represented by one individual and to reduce the dominance of the most abundant species (R Development Core Team, 2009). In order to investigate similarities in standing stock between sites and habitats a two-way crossed PERMANOVA (Bray-Curtis similarity, 999 permutations) test, analogous to the univariate GLM, was carried out using the vegan library (Oksanen, 2011) in the R environment (Clarke and Warwick, 1994). Using Primer 6 (Clarke and Warwick, 1994) differences in communities between sites and habitats were visualised with a non-metric multidimensional scaling (MDS) and hierarchical clustering that was overlain onto the MDS plot. A one-way SIMPER analysis was run in Primer 6, based on Bray-Curtis similarity with a cut off for low contributions at 90%. This analysis shows a) the % similarity of the assemblages between individual transects, factored by site and habitat respectively; and b) the % average dissimilarity between sites, in terms of species composition.

2.3.1. Feeding guilds

Operational taxonomic units were assigned to the following feeding guilds: a) deposit feeders, b) suspension feeders, c) omnivores and d) carnivores. For a large number of OTUs the feeding guild was based either on the literature or on direct observations by the authors during cruises to the study area. Omnivores were assigned also in cases were the identification was not detailed enough to assign a feeding guild with any certainty. After all OTUs were assigned a feeding guild, the total number representing each feeding guild was calculated together with their % contribution for each habitat within each site. The OTUs were

ranked by abundance in order to determine whether the modes of feeding showed a pattern within the study area. The most abundant OTU from each site was superimposed on a MDS plot, together with its feeding guild and its % contribution to the community within each respective transect. Note that for these calculations only taxonomic units with a count > 0 were included.

2.4. Sediment granulometry

Samples were collected at each site during the RRS *James Cook* cruise JC011 in 2007 (Priede, 2007) as part of a Megacore survey. Sediment grain size distribution was analysed at the National Oceanography Centre, Southampton. Each site was analysed in 1 cm increments from the surface down to 5 cm sediment depth. The sediment analysis was carried out using laser diffraction with a Malvern Mastersizer 2000 (beam length 2.35, absorption 0.01, dispersion 1.330). Results were categorised using the Wentworth grain size scale.

3. Results

3.1. Environment

At all four sites the seabed was mainly soft sediment. Images revealed differences in pteropod thanatocoenoses between sites. Pteropod shells were frequently observed at the southern sites but virtually absent in the north (Fig. 2). Shells were densely distributed throughout most transects in the SW. At the SE site they were more common on flat habitats, with a patchy distribution on slopes. Sediment ripples were observed during initial ROV observations at the SW site but none were seen during the transect runs. As we had targeted flat and gently sloping areas, rocky substratum was very rare, with only occasional observations of cobbles / boulders. The top 5 cm of sediment in the core samples ranged from clay to coarse sand, with fine silt predominating (> 95%) at all sites (Fig. 3).

3.2. Standing stock

In total 57,356 individual organisms, representing 154 OTUs, from nine different phyla (Table 2, Sup 1), were recorded across 32,000 m² of seafloor (Fig. 4). Overall, the standing stock was dominated by echinoderms, followed by poriferans, foraminifera, and cnidarians (Table 2). Annelid counts were low; those observed were very small and only larger species, such as Polynoidae (Family) indet, could be

identified with certainty in the video footage; arthropod counts were also low. However, many of the arthropods were highly mobile and, although not counted, were observed in forward-looking cameras moving away from the imaged area.

The standing stock differed significantly between sites (GLM (quasi-Poisson): L-ratio = 11.59, df = 3, p < 0.001) and was substantially higher in the north (total of 42,292 individuals per 16,000 m²) than in the south (15,064 individuals per 16,000 m²). East-west differences in standing stock were not so pronounced or significantly different (GLM (quasi-Poisson): L-ratio = 0.76, df = 1, p = ns), although greater in the east (total of 34,912 individuals per 16,000 m²) than in the west (22,444 individuals per 16,000 m²). The standing stock was not affected by slopes alone (GLM (quasi-Poisson): L-ratio = 3.30, df = 1, p = 0.07), but by the interaction of sites and slopes (GLM (quasi-Poisson): L-ratio = 11.04, df = 3, p = 0.01). This indicates that the observed difference in standing stock between slopes was site dependent, driven by the approximately four-fold lower standing stocks at the 10° slopes than the flat areas at the southern sites. No clear pattern was seen in the north, with standing stocks approximately four-fold higher in the flat areas compared with the sloping areas in the NE and four-fold lower in the flat areas compared with the sloping areas in the NW.

The abundant phyla differed between sites (Tables 2, 3). The NW site was characterised by large numbers of sponges, echinoderms and foraminifera. Sponges were dominated by Hexactinellida (Class) sp. A and Hexactinellida (Class) indet. in all transects (Supplementary material S1). One transect at the NW site (transect: NW3) had unusually high densities of sponges, including numerous individuals of *Pheronema* sp., Rossellidae sp. A and Hexactinellida (Class) sp. B. Echinoderms at the NW site were principally represented by the echinoids *Urechinus naresianus* and the Urechinidae/Heminasteridae complex, and by the ophiuroids Ophiuroidea (Class) indet., Ophiuroidea (Class) sp. A and Ophiuroidea (Class) sp. B. Foraminifera at the NW site were represented by high densities of the xenophyophore *Syringammina* sp. and the large discoidal miliolid *Discospirina tenuissima*, particularly at NW3. The largest standing stock of echinoderms was at the NE site, which was characterised by the aggregating holothurian *Kolga nana*, and the irregular echinoid *Pourtalesia* (Genus) indet. A. The sponge Hexactinellida (Class) sp. A was also common at the NE site. The sponges Porifera (Phylum) indet. and Rossellidae sp. A, and the foraminiferan *D. tenuissima*, occurred in high densities at the SW site. Finally, the SE site was characterised by the echinoid *Pourtalesia* (Genus) indet. and again by *D. tenuissima* (Table 2).
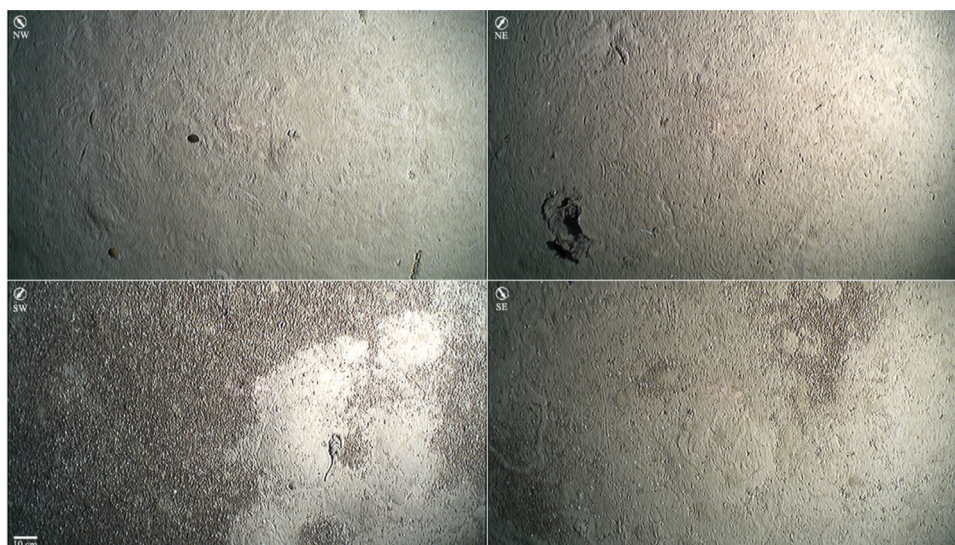

Fig. 2. Images representing typical seabed at each site (indicated on figure), including the pteropod thanatocoenoses.
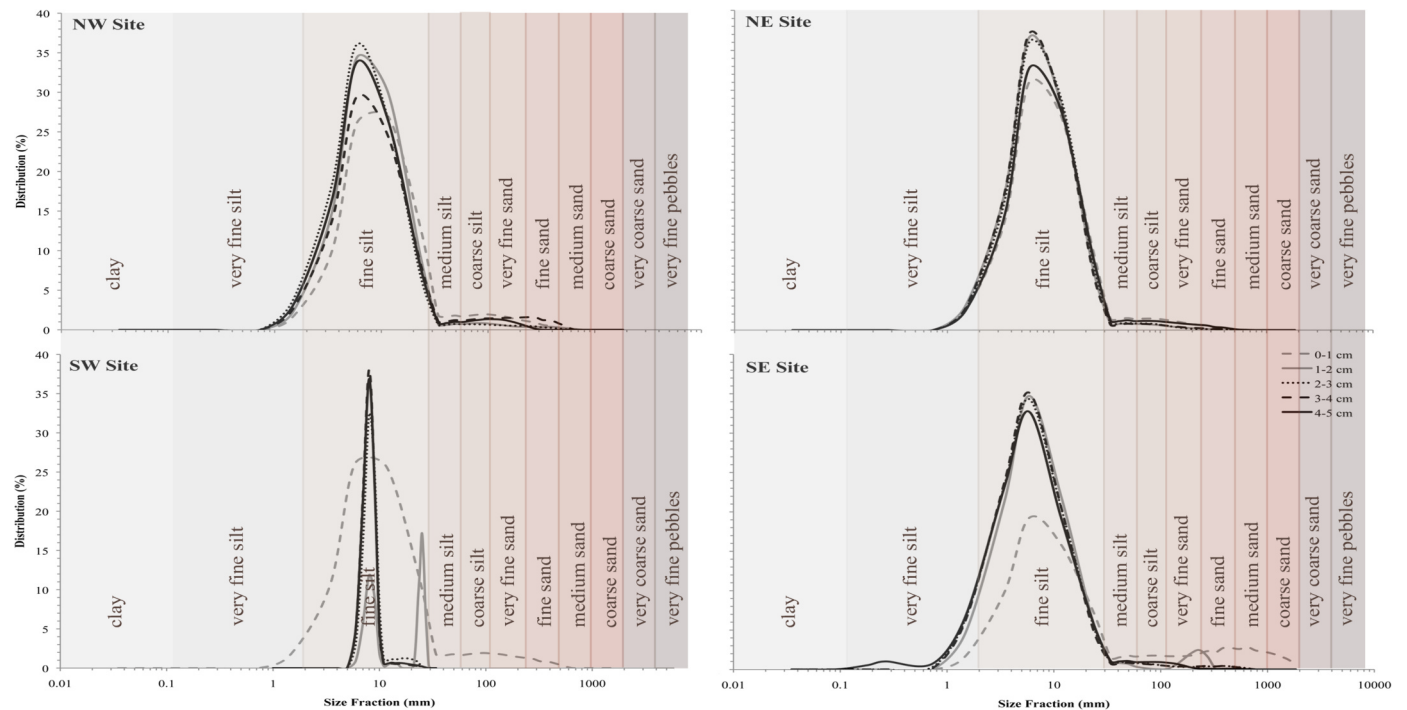
Fig. 3. Distribution of the sediment grain sizes from Megacore samples. Size fractions for each cm displayed for the first five cm at every site. Note that the size fractions are displayed on a logarithmic scale.

Table 2
The standing stock (individuals per 8000 m^2 and the percentages of the total at each site) of different phyla at each site.

Phylum	NW site	NE site	SW site	SE site	Total
Echinodermata	4049 (27%)	24,367 (90%)	864 (12%)	3870 (50%)	33,150
Porifera	7044 (47%)	1384 (5%)	1480 (20%)	814 (11%)	10,722
Foraminifera	2945 (20%)	1070 (4%)	3759 (51%)	2143 (28%)	9917
Cnidaria	447 (3%)	254 (1%)	959 (13%)	533 (7%)	2193
Hemichordata	33 (< 1%)	60 (< 1%)	120 (2%)	221 (3%)	434
Nemertea	352 (2%)	6 (< 1%)	4 (< 1%)	6 (< 1%)	368
Annelida	135 (1%)	45 (< 1%)	29 (< 1%)	21 (< 1%)	230
Arthropoda	57 (< 1%)	29 (< 1%)	71 (1%)	58 (1%)	215
Mollusca	7 (< 1%)	5 (< 1%)	83 (1%)	22 (< 1%)	117
Bryozoa	2 (< 1%)	0 (0%)	3 (< 1%)	0 (0%)	5
Total	15,071	27,221	7373	7691	57,356

3.3. Species richness

There were clear differences in species richness between the sites and habitats. The western sites (NW and SW) had higher species richness than the eastern (Fig. 5). Species richness was highest at the SW site and lowest at the NE site. The sloped habitats did not have consistently higher or lower species richness than the flat sites.

3.4. Community composition

Five distinct clusters were differentiated based on the community composition within each transect (Fig. 6). Northern transects grouped by site, with an 80% similarity in species composition within each site. Transects from the southern sites formed three further distinct groups. The majority of the southern transects (13) grouped into a main cluster, but two SE transects (SE2 & SE1) and one SW transect (SW6) were distinct. The community composition of transects SE1 and SE2 shared only about 20% similarity with other transects from the SE site (Fig. 6). This distinction was driven by high abundances of *Pourtalesia* indet. and to a lesser extent by *D. tenuissima*. The distinction of transect SW06 from the main southern cluster was driven by a greater abundance of sponges. Several meters of continuous hard rock substrata in the form of

boulders and pebbles were observed on the seabed at SW6. This may explain the faunal differences, as other transects only revealed soft sediment communities (Fig. 6).

There was a clear distinction between communities from the north and south. Both northern sites were also clearly distinct from one another and shared < 40% similarity in community composition (Fig. 6). The community composition did not differ between habitats at the NW site. The separation of transects based on their community composition reflected their geographic separation (Fig. 1). The NW3 transect had unusually high densities with over 11,000 individuals in 1000 m^2 of seafloor, while all other transects averaged 700 individuals over the same area. At the NE site, communities on flat (0–2°) and sloped (10°) areas were distinct. Within each of these areas, the community composition showed > 60% similarity, while between them, the similarity ranged between 40% and 60%. The similarity in community composition between the majority of southern transects was greater (> 40%) than that within the NW and NE sites (Fig. 6). Overall, the community composition varied significantly between sites (PERMANOVA: Pseudo-F = 7.75, df = 3, p < 0.001), habitats (PERMANOVA: Pseudo-F = 6.67, df = 1, p < 0.001) and the interaction between sites and habitats (Pseudo-F = 3.48, df = 3, p < 0.001). At the southern sites the distinctions between communities were driven by habitat type rather than
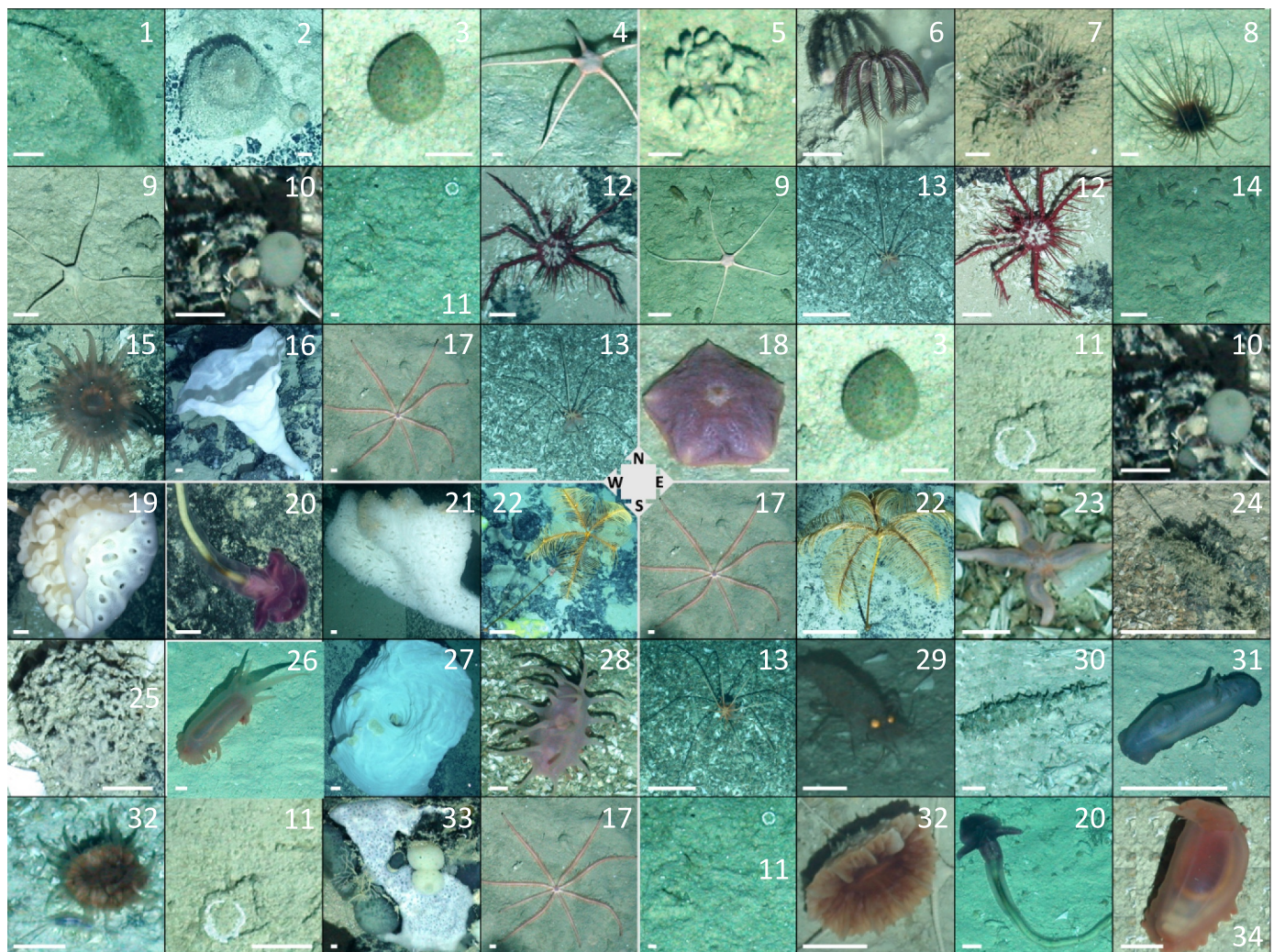
Fig. 4. Images representing common fauna of the area. Centre indicating compass directions, highlighting the 4 sites. Scale bar in each image represents 2 cm. In order of abundance within each site, left to right. 1. Hydoidolina sp. A, 2. Hexacteinellida sp. C, 3. *Urechinus naresianus*, 4. Ophiuroide sp. A, 5. Xenophyophoroidea (suborder) indet., 6. Bourgueticrinidae sp., 7. Pourtalesia indet, 8. Cerianthidae sp. A, 9. Ophiuroidea sp. B, 10. Hexacteinellida sp. A, 11. *Discospirina tenuissima*, 12. Lithodididae sp, *13. Colossendeis colosse*a, 14. *Kolga nana*, 15. Actinaria sp., 16. Hexactinellida sp. D, 17. *Freyella* sp., 18. Hymenaster sp. A, 19. Hexactinellida sp. E, 20. *Yoda purpurata,* 21. Hexactinellida sp. F, 22. *Anachalypsicrinus nefertini*, *23. Hydrasterias sexradiata*, 24. Hydroidolina sp. B, *25. Syringammina* sp., 26. *Peniagone islandica*, 27. Hexactinellida sp. D, 28. *Deima validum, 29. Glyphocrangon sculpta, 30.* Maldanidae (Family) indet., 31. *Psychropotes* sp. nov., *32. Flabellum angulare, 33.* Hexactinellida sp. H, 34. Elpidiidae indet.

site. However, within particular habitats, communities were different between the eastern and western sites (Fig. 6).

3.5. Species distributions between sites and habitats

OTUs contributing to the dissimilarity in species composition between sites included three taxa that were common to all sites: Porifera (Phylum) indet., Hexactinellida (Class) indet., and *Discospirina tenuissima*. Hydroidolina (Subclass) indet. contributed to the dissimilarity in species composition at the NW, SW and SE sites, but not at the NE site, while *Pourtalesia* (Genus) indet. was important at the eastern sites, and Holothurian (Class) indet. at the NE and SW (Table 3).

Between habitats, taxa contributing to differences were similar at the northern sites. Habitats at the NW site had the same OTUs as the NE, but they differed in rank. Except for Ophiuroidea (Class) indet. (flat habitat) and Hexactinellida (Class) indet. (10° slope habitat), taxa were the same between habitats at the NE sites. Only two OTUs were common to different habitats at the southern sites - at the SW site these were Hydroidolina (Subclass) indet., and Porifera (Phylum) indet. and at the SE site *D. tenuissima* and Porifera (Phylum) indet.) - while three taxa contributed uniquely to the different habitats (Table 3). Overall, the species composition in flat habitats was more similar between the sites (66.7%) than the 10° slope habitats (59.3%).

The total numbers of OTUs were approximately the same between the sites (total OTU: 86 NE, 103 NW, 73 SE, 104 SW). However, there were different numbers of unique OTUs between the sites, with only 1 at the SE, 10 at the NE, 16 at the SW and 21 at the NW (Table 4). The sloped areas (10°) had generally more unique OTUs than the flat areas (with the exception of the SE site; Table 5).

The northern, southern, eastern and western sites all showed similar levels of species richness and species accumulation rates, with the most distinct OTUs to the west of the MAR (total OTUs: north 130, south 116, east 102, west 140). The eastern sector had 3 OTUs that were not present in the west, and the western sector had 15 OTUs that were not present in the east. Both the northern and southern sectors had 7 OTUs that were not present in the other sector.

3.6. Feeding guilds

Deposit and suspension feeders accounted for 81% of the taxonomic

Table 3

SIMPER results for each site, showing the 11 most important taxonomic units (TU) that differentiate sites, with the % contribution of each TU. It also shows differences in OTU contributions between habitats.

Habitat	NW site	%	NE site	%	SW site	%	SE site	%
All	*Urechinus naresianus*	15.2	*Kolga nana*	39.3	Porifera (Phylum) indet.	16.5	*Discospirina tenuissima*	12.9
	Urechinidae/Hemimasteridae complex	12.5	Urechinidae/Hemimasteridae complex	8.0	*Discospirina tenuissima*	12.7	Porifera (Phylum) indet.	11.0
	Porifera (Phylum) indet.	11.5	Ophiuroidea (Class) indet.	7.1	Hydroidolina (Subclass) indet.	7.7	Hydroidolina (Subclass) indet.	7.6
	Hexactinellida (Class) indet.	7.5	*Pourtalesia* (Genus) indet.	6.1	*Flabellum angulare*	5.7	*Yoda purpurata*	7.1
	Ophiuroidea (Class) indet.	7.2	Porifera (Phylum) indet.	5.9	Hexactinellida (Class) indet.	4.7	*Flabellum angulare*	5.4
	Ophiuroid sp. A	4.7	Hexactinellida (Class) indet.	5.5	*Yoda purpurata*	3.8	Hexactinellida (Class) indet.	5.3
	Discospirina tenuissima	4.1	*Urechinus naresianus*	3.0	*Peniagone* (Genus) indet.	3.5	*Hydraasterias sexradiata*	4.7
	Hydroidolina (Subclass) indet.	3.5	*Discospirina tenuissima*	2.1	Holothurian (Class) indet.	3.5	*Peniagone* (Genus) indet.	4.4
	Hydroidolina sp. A	3.3	*Hymenaster* (Genus) indet. A	2.0	Scaphopod (Class) indet.	3.2	Cnidaria (Phylum) indet.	3.8
	Hexactinellida sp. A	3.2	Holothurian (Class) indet.	2.0	Elpidiidae (Family) indet.	3.0	*Pourtalesia* (Genus) indet.	3.6
	Ophiuroidea sp. B	2.7			*Syringammina* sp.	2.9	*Glyphocrangon sculpta*	2.5
Flat	*Urechinus naresianus*	14.0	*Kolga nana*	26.9	*Discospirina tenuissima*	23.2	*Discospirina tenuissima*	15.0
	Urechinidae/Hemimasteridae complex	9.3	*Pourtalesia* (Genus) indet.	9.5	Porifera (Phylum) indet.	10.9	*Pourtalesia* (Genus) indet.	14.6
	Porifera (Phylum) indet.	9.2	Urechinidae/Hemimasteridae complex	7.0	*Flabellum angulare*	8.7	Hydroidolina (Subclass) indet.	8.0
	Ophiuroidea (Class) indet.	9.0	Porifera (Phylum) indet.	6.1	Hydroidolina (Subclass) indet.	5.5	*Yoda purpurata*	7.1
	Hexactinellida (Class) indet.	7.1	Ophiuroidea (Class) indet.	5.6	*Syringammina* sp.	4.5	Porifera (Phylum) indet.	6.1
10°	Urechinidae/Hemimasteridae complex	16.7	*Kolga nana*	19.7	Porifera (Phylum) indet.	22.3	Porifera (Phylum) indet.	16.8
	Urechinus naresianus	14.2	Porifera (Phylum) indet.	8.6	Hydroidolina (Subclass) indet.	8.4	Hexactinellida (Class) indet.	8.3
	Porifera (Phylum) indet.	12.6	*Pourtalesia* (Genus) indet.	8.5	Hexactinellida (Class) indet.	7.8	*Flabellum angulare*	8.0
	Hexactinellida (Class) indet.	7.3	Urechinidae/Hemimasteridae complex	8.1	Scaphopod (Class) indet.	6.2	*Discospirina tenuissima*	8.0
	Ophiuroidea (Class) indet.	6.4	Hexactinellida (Class) indet.	6.8	Elpidiidae (Family) indet.	6.0	*Peniagone* (Genus) indet.	5.5

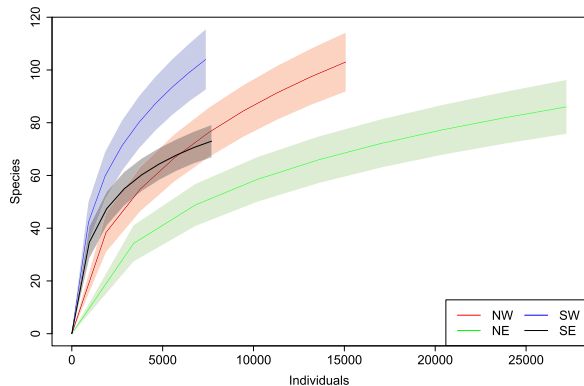**Fig. 5.** Individual-based species accumulation curves for each site. Shaded polygons represent 95% confidence intervals.

Fig. 6. Multidimensional Scaling Plot showing differences in community composition between sites and habitats. Each point represents the community composition of a single transect. Sites are indicated by colours, slope levels are indicated by shapes. Stress for two-dimensional MDS is 0.16.

units across sites (Table 6) and the remainder were omnivores and carnivores. When ranked by abundance, a clear separation could be made between transects that were dominated by either deposit or suspension feeders. In the south, communities dominated by suspension feeders were found in 10° slope habitats, while flat habitats were dominated by deposit feeders, regardless of whether they were to the east or west of the ridge. A clear differentiation of habitat types based on megafaunal feeding modes was not possible in the north, where all transects, except NW11 and NW03, were dominated by a deposit feeder.

4. Discussion

4.1. Differences North & South of the CGFZ

The Charlie-Gibbs Fracture Zone, a seabed feature, coincides with a surface oceanographic feature, namely the position of the northern edge of Sub-Polar Front (Longhurst, 2007; Agostini et al., 2009; Priede
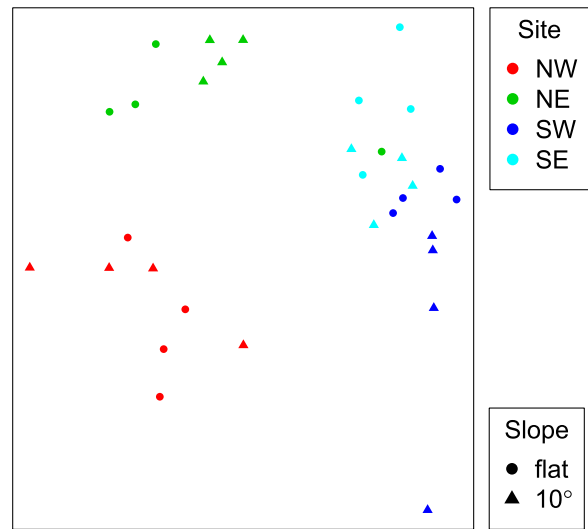
Table 4

Summary statistics for each site (with both slope levels combined). Density: number of organisms per meter squared, S: total number of OTUs observed, ESn (7542): Estimated OTUs in 7542 individuals, Unique OTUs: number of OTUs only found at that site.

Site	Density	S	ESn	Unique OTUs
NW	1.88	103	75	21
NE	3.40	86	50	10
SW	0.92	104	104	16
SE	0.96	73	72	1

Table 5

Summary statistics for each site (separate slope levels). Density: number of organisms per meter squared, S: total number of OTUs observed, Unique OTUs: number of OTUs only found at that site.

Site	Density	S	Unique OTUs
NW flat	0.82	69	6
NW 10°	2.95	82	10
NE flat	5.36	65	2
NE 10°	1.45	65	7
SW flat	1.49	70	6
SW 10°	0.36	85	8
SE flat	1.57	61	1
SE 10°	0.35	52	0

Table 6

The feeding guilds of megafauna at the Mid-Atlantic Ridge. Total number of taxonomic units and percentage of total at each site separated by feeding type.

Feeding guild	NW site	NE site	SW site	SE site	Total
Deposit feeders	33 (32%)	33 (38%)	36 (35%)	28 (38%)	53
Suspension feeders	51 (50%)	31 (36%)	49 (47%)	29 (40%)	72
Omnivores	8 (8%)	9 (10%)	6 (6%)	6 (8%)	11
Carnivore	11 (11%)	13 (15%)	13 (12%)	10 (14%)	18
Total	103	86	104	73	154

et al., 2013a). The northern and southern megafaunal communities are only 20% similar (Fig. 6), suggesting that the CGFZ and/or SPF, which separate them, may exert some influence on their composition. This may be a result of reduced connectivity across the topographically complex fracture system, combined with the geographical separation between our northern and southern sites. The role of different regimes associated with the SPF also cannot be excluded. Distinct community compositions at northern and southern ECOMAR sites were reported for fish (King et al., 2006; Bergstad et al., 2008b; Cousins et al., 2013; Linley et al., 2013), megafauna inhabiting steep slopes (Bell et al., 2016), enteropneusts (Jones et al., 2013), bentho-pelagic amphipods (Horton et al., 2013), cephalopods (Vecchione et al., 2010) and zoo-plankton (Gaard et al., 2008; Hosia et al., 2008). It is assumed that this divide is driven by changes in the quality (Kiriakoulakis et al., 2001; Wigham et al., 2003) and quantity (Lauerman and Kaufmann, 1998; Soltwedel et al., 2009) of available organic material caused by differences in water masses north and south of the SPF. Recent studies based on satellite data show higher primary production north of the CGFZ (Tilstone et al., 2014), suggesting that a greater quantity of material reaches the seafloor at our northern sites (Lutz et al., 2007). However, these differences in surface productivity were not reflected in the quantity of the annual material flux (Abell et al., 2013). In addition, temperatures, salinity and dissolved bottom-water oxygen concentrations are all similar across the fracture zone (Gooday et al., 2013; Priede et al., 2013a). Moreover, several benthic faunal studies report no north to south differences in community composition (Alt et al., 2013) or the occurrence of particular species (Gooday et al., 2013).

Although the quality of the material flux was not analysed directly, inferences from modelled source regions, based on sediment trap data from around 2400 m depth, imply potential differences in particle composition between areas to the north and south of the CGFZ/SPF (Abell et al., 2013). The trajectory of particles indicates overlapping source regions in the south, and discrete source regions at both northern sites, thus mirroring the pattern observed for the species compositions of benthic megafauna (Fig. 6). Upper ocean communities appear different either side of the Sub-Polar Front, the northern edge of which lies just south of the CGFZ (Letessier et al., 2011, 2012; Priede et al., 2013a). Moreover, differences in sedimentary organic matter were also apparent in sediment samples collected during all cruises (Abell et al., 2013). In the south, phytodetritus was present during all

sampling seasons, while a thin phytodetritus layer was only observed once (during spring) in the north. This suggests that different processes take place in these two areas, particularly since there is no evidence for a distinct north/south contrast in organic matter flux (Abell et al., 2013).

The distinct differences in megabenthic communities were driven by significant differences in overall standing stock between the sites and differences in the taxa observed. For example, the echinoids *Urechinus naresianus* and the Urechinidae/Hemimasteridae complex, and the sponge Hexactinellida sp. A, were commonly sighted at the northern sites but virtually absent in the south. Conversely, the cnidarian *Flabellum angulare*, the enteropneust *Yoda purpurata*, and the arthropods *Munidopsis rostrata* and *Glyphocrangon sculpta* were common in the south, but rare in the north. Finally, the pteropod thanatocoenoses, which could potentially increase habitat heterogeneity (Zajac, 2008), were confined to the southern sites.

Another environmental factor that may contribute to community differences is the sediment composition (Rex, 1981; Auster et al., 1991; Bett et al., 2001). Megacore samples revealed differences in deeper layers (Priede, 2007, 2009; Priede and Bagley, 2010). The northern sediment showed a distinct layer at about 15 cm, after which the sediment changed from a surficial light brown to a darker layer (about 5 cm thick), lying on top of a grey deep layer. In the south the sediment tended to be homogenous in the megacorers, without any banding. Although these observations are more relevant to infauna, their distribution could have a secondary effect on epibenthic fauna. A granulometric analysis of the top 5 cm of sediment also revealed that, although the sediment was dominated by fine silts at all sites, there were localised differences (Fig. 3). Variation in the quality or quantity of organic matter in sediments are common (Wolff et al., 2011), particularly in areas with variable local hydrography and topography like the MAR, and are important in the ecology of many benthic species, such as holothurians (Wigham et al., 2008). It is therefore plausible that the localised variations observed in the sediment affect the distribution of some epifauna.

4.2. East to West patterns across the MAR

Distinct differences in megafaunal communities were observed in the present study between the west and east sites to the north of the CGFZ and SPF. This was particularly evident in the occurrence of aggregations of *Kolga nana* only at the NE site and high abundances of Ophiuroidea (Class) indet. and Nemertea (Phylum) indet. only at the NW site. In contrast, the two southern sites were much more similar, despite being situated on opposite sides of the ridge (Fig. 1). This suggests that an ecological barrier only exists in this area of the MAR to the north of the CGFZ and SPF and not to the south. This stands in contrast to previous studies that consider the MAR a biogeographic barrier only south of the CGFZ owing to the differences in surface productivity (Longhurst, 2007); and both north and south of the CGFZ as a result of diel migration and seasonal blooms (Beaugrand et al., 2001). Gebruk et al. (2010) reported significant differences in bathyal benthic fauna east and west from the ridge in two transects: south east of CGFZ (51°N) and much further south, north of the Azores (43°N). The percentage of species occurring only east or only west of the ridge in these two areas was 75% and 72% respectively. At the same time, some authors do not consider the ridge a biogeographic barrier at all owing to similarities in temperature, salinity and the amount of dissolved oxygen across the MAR (Agostini et al., 2009).

Current movement can impact species richness when moderate currents enhance food supply by delivering organic matter and stimulating bacterial production (Levin et al., 2001; Palardy and Witman, 2011). However, while water masses cross the ridge from west to east (Abell et al., 2013; Priede et al., 2013a), no noticeable difference in current speed was measured between the west and east sites at depths of about 2500 m, thus making an enhanced local material flux through

currents unlikely (Abell et al., 2013).

In this study, species richness was higher at the western sites, both north and south of the CGFZ. Species richness was approximately the same as found in other studies in the same region (154 spp. here; 153 spp. in Alt et al., 2013 and 192 spp. in Gebruk et al., 2010). Interestingly, species richness was lowest at the site with the highest density (NE). This may be caused by small holothurians, such as *Kolga nana*, forming large temporary aggregations (Billett and Hansen, 1982; Rogacheva et al., 2013), presumably in response to a food resource, potentially reducing the available resource for other deposit feeders. In another study, Gebruk et al. (2010) found higher species richness to the north west (102 spp.) of the CGFZ than to the SE (spp.70). The pattern of higher species richness in the northern sites appears to hold in the fauna of steep slopes in the same region as this study but there was higher richness in the east than the west of the MAR (Bell et al., 2016).

4.3. Within-site habitat complexity

Most transects within each site to the north of the CCFZ had similar community compositions, but the NE and NW sites themselves were distinct (Fig. 6). This scale-dependent decrease in community similarity is typical of beta-diversity gradients (McClain et al., 2011; Alt et al., 2013). To the south of the CGFZ, the within-site variability in community composition was greater than observed at the northern sites, and there was little distinction between communities to the east and west of the ridge. At the SW site particularly, the community composition differed between the slope types (Fig. 6). Prior to this study it was hypothesised that flatter areas would have higher organic matter availability as a result of lower lateral transport and local current speeds, potentially increasing species richness and standing stock, at least for deposit feeders (Jones et al., 2013). Although differences in standing stock were observed between slope types, no clear pattern could be discerned. The observed increase in standing stock on some slopes was site specific, as were observed differences in community composition between habitats. In the absence of a clear trend between standing stock, community composition and slope, additional factors appear to contribute to the differences in benthic community compositions.

Local habitat complexity was increased by the pteropod thanatocoenoses (Zajac, 2008) and biotic structures, such as xenophyophores (Levin, 1994; Hughes and Gooday, 2004) and sponges (Buhl-Mortensen et al., 2010), all of which could potentially influence community composition (Levin and Dayton, 2009). Although xenophyophores were present throughout, pteropod shells covered the seafloor at the southern sites, but were virtually absent in the north. Although the distribution of pteropod shells was similar across both habitats in the SW area, accumulations were denser on the flat habitat than on the sloped habitat in the SE area. Despite these differences in pteropod shell cover between the two habitats, community composition in the south was similar, suggesting that the thanatocoenoses are unlikely to have a strong effect on megafaunal community composition in this case.

Patterns in dominant feeding mode were not consistent between sites (Table 6), and the northern sites differed strongly in the number of filter and deposit feeders. Our data reveal very few environmental differences between them. It is possible that small-scale topography or patterns in current flow not discernible from our data were responsible for these patterns. All the filter feeders that we observed were fragile, implying that they were only exposed to weak currents (Christiansen and Thiel, 1992). Except for one outlier (transect 11 at the NW site), the transects with the greatest elevations were dominated by suspension feeders, while all others were dominated by deposit feeders. This may be a result of increased availability of fresh particulate organic matter, which acts as a driver for the community composition and dominant feeding mode at very localised scales.

In conclusion, the MAR appears to be important in structuring the Atlantic benthos. It is already known that the MAR greatly increases the

bathyal area of the ocean (Niedzielski et al., 2013) and enhances benthic biomass significantly in the Atlantic (Priede et al., 2013b). Here, we show that in an area of the northern MAR, a fracture zone in the ridge, combined with Sub-Polar Front and the ridge itself, appear to act as ecological barriers for megafaunal species and that significantly different megafaunal assemblages are observed either side of these barriers. However, these patterns are likely not consistent along the length of the ridge. Even in this study, where only a small proportion of the whole ridge was analysed, we see differences in the role of the ridge in separating megafaunal communities in different ridge segments, with more separation north of the CGFZ and less to the south. Our results suggest that the MAR greatly increases habitat heterogeneity and harbours a wide range of megafaunal taxa. This study represents one of the largest quantitative studies of megafaunal assemblages associated with the MAR. Additional similar investigations are required to understand better the importance of this feature for benthic biodiversity at a regional scale.

Competing interests statement

Declarations of interest

None.

Appendix A. Supporting information

Supplementary data associated with this article can be found in the online version at doi:10.1016/j.dsr.2018.12.006

References

Abell, R., Brand, T., Dale, A., Tilstone, G., Beveridge, C., 2013. Variability of particulate flux over the Mid-Atlantic Ridge. Deep-Sea Res. Part II: Top. Stud. Oceanogr. 98, 257–268.

Agostini, V.N., Arico, S., Escobar-Briones, E., Malcolm, C., Cresswell, I., Gjerde, K., Grant, S., Niewijk, D.J.A., Polacheck, A., Rice, J., Roff, J., Scanlon, K.M., Smith, C., Spalding, M., Tong, E., Vierros, M., Watling, L., 2009. Global Open Oceans and Deep Seabed (GOODS) - Biogeographic Classification. IOC Technical Series 84, Intergovernmental Oceanographic Commission.

Alt, C.H.S., Rogacheva, A., Boorman, B., Hughes, J.A., Billett, D.S.M., Gooday, A.J., Jones, D.O.B., 2013. Trawled megafaunal invertebrate assemblages from bathyal depth of the Mid-Atlantic Ridge (48°–54°N). Deep-Sea Res. Part II: Top. Stud. Oceanogr. 98, 326–340.

Auster, P.J., Malatesta, R.J., LaRosa, S.C., Cooper, R.A., Stewart, L.L., 1991. Microhabitat utilization by the megafaunal assemblage at a low relief outer continental shelf site - Middle Atlantic Bight, USA. J. Northwest Atl. Fish. Sci. 11, 59–69.

Beaugrand, G., Ibañez, F., Lindley, J.A., 2001. Geographical distribution and seasonal and diel changes in the diversity of calanoid copepods in the North Atlantic and North Sea. Mar. Ecol. Prog. Ser. 219, 189–203.

Beaulieu, S.E., 2001. Life on glass houses: sponge stalk communities in the deep sea. Mar. Biol. 138 (4), 803–817.

Bell, J.B., Jones, D.O.B., Alt, C.H.S., 2013. Lebensspuren of the bathyal Mid-Atlantic Ridge. Deep-Sea Res. Part II: Top. Stud. Oceanogr. 98, 341–351.

Bell, J.B., Alt, C.H.S., Jones, D.O.B., 2016. Benthic megafauna on steep slopes at the Northern Mid-Atlantic Ridge. Mar. Ecol. 37 (6), 1290–1302.

Bergstad, O.A., Falkenhaug, T., Astthorsson, O.S., Byrkjedal, I., Gebruk, A.V., Piatkowski, U., Priede, I.G., Santos, R.S., Vecchione, M., Lorance, P., Gordon, J.D.M., 2008a. Towards improved understanding of the diversity and abundance patterns of the mid-ocean ridge macro-and megafauna. Deep-Sea Res. Part II: Top. Stud. Oceanogr. 55, 1–5.

Bergstad, O.A., Menezes, G., Høines, Å.S., 2008b. Demersal fish on a mid-ocean ridge: distribution patterns and structuring factors. Deep-Sea Res. Part II: Top. Stud. Oceanogr. 55, 185–202.

Bett, B.J., Malzone, M.G., Narayanaswamy, B.E., Wigham, B.D., 2001. Temporal variability in phytodetritus and megabenthic activity at the seabed in the Northeast Atlantic. Progress. Oceanogr. 50 (1–4), 349–368.

Billett, D.S.M., Hansen, B., 1982. Abyssal aggregations of *Kolga hyalina* Danielssen and Koren (Echinodermata: Holothuroidea) in the northeast Atlantic Ocean: a preliminary report. Deep-Sea Res. 29 (7A), 799–818.

Buhl-Mortensen, L., Vanreusel, A., Gooday, A.J., Levin, L.A., Priede, I.G., Buhl-Mortensen, P., Gheerardyn, H., King, N.J., Raes, M., 2010. Biological structures as a source of habitat heterogeneity and biodiversity on the deep ocean margins. Mar. Ecol. 31, 21–50.

Christiansen, B., Thiel, H., 1992. Deep-sea epibenthic megafauna of the northeast Atlantic: abundance and biomass at three mid-ocean locations estimated from photographic transects. Deep-Sea Food Chains Glob. Carbon Cycle 20, 125–138.

Clarke, K.R., Warwick, R.M., 1994. Change in Marine Communities - An Approach to Statistical Analysis and Interpretation. Plymouth Marine Laboratory.

Colwell, R.K., Mao, C.X., Chang, J., 2004. Interpolating, extrapolating, and comparing incidence-based species accumulation curves. Ecology 85, 2717–2727.

Cousins, N.J., Shields, M.A., Crockard, D., Priede, I.G., 2013. Bathyal demersal fishes of the Charlie Gibbs fracture zone region (49-54°N) of the Mid-Atlantic Ridge, I: Results from trawl surveys. Deep-Sea Res. Part II: Top. Stud. Oceanogr. 98, 388–396.

Fox, J., Weisberg, S., 2011. An R Companion to Applied Regression, 1st edition. SAGE.

Gaard, E., Gislason, A., Falkenhaug, T., Søiland, H., Musaeva, E., Vereshchaka, A., Vinogradov, G., 2008. Horizontal and vertical copepod distribution and abundance on the Mid-Atlantic Ridge in June 2004. Deep-Sea Res. Part II: Top. Stud. Oceanogr. 55, 59–71.

Gebruk, A., Budaeva, N.E., King, N., 2010. Bathyal benthic fauna of the Mid-Atlantic Ridge between the Azores and the Reykjanes Ridge. J. Mar. Biol. Assoc. 90, 1–14.

Glover, A.G., Gooday, A.J., Bailey, D.M., Billett, D.S.M., Chevaldonné, P., Colaço, A., Copley, J., Cuvelier, D., Desbruyères, D., Kalogeropoulou, V., Klages, M., Lampadariou, N., Lejeusne, C., Mestre, N.C., Paterson, G.L.J., Perez, T., Ruhl, H.A., Sarrazin, J., Soltwedel, T., Soto, E.H., Thatje, S., Tselepides, A., van Gaever, S., Vanreusel, A., 2010. Temporal Change in Deep-sea Benthic Ecosystems: A Review of the Evidence from Recent Time-series Studies Vol. 58. Elsevier, Ch., pp. 1–95.

Gooday, A.J., Alt, C.H.S., Jones, D.O.B., Shale, D., Marsden, K., Brasier, M.D., 2013. The ecology and biogeography of *Discospirina tenuissima* (foraminifera) in the Atlantic and Indian oceans. Deep-Sea Res. Part II: Top. Stud. Oceanogr. 98, 301–314.

Grassle, J.F., 1991. Deep-sea benthic biodiversity. Bioscience 41 (7), 464–469.

Gray, J.S., 2000. The measurement of marine species diversity, with an application to the benthic fauna of the Norwegian continental shelf. J. Exp. Mar. Biol. Ecol. 250 (1–2), 23–49.

Gutt, J., Piepenburg, D., 2003. Scale-dependent impact on diversity of Antarctic benthos caused by grounding of icebergs. Mar. Ecol. Prog. Ser. 253, 77–83.

Horton, T., Thurston, M.H., Duffy, G.A., 2013. Community composition of scavenging amphipods at bathyal depths on the Mid-Atlantic Ridge. Deep-Sea Res. Part II: Top. Stud. Oceanogr. 98, 352–359.

Hosia, A., Stemmann, L., Youngbluth, M., 2008. Distribution of net-collected planktonic cnidarians along the northern Mid-Atlantic Ridge and their associations with the main water masses. Deep-Sea Res. Part II: Top. Stud. Oceanogr. 55, 106–118.

Hughes, J.A., Gooday, A.J., 2004. Associations between living benthic foraminifera and dead tests of *Syringammina fragilissima* (Xenophyophorea) in the Darwin Mounds region (NE Atlantic). Deep-Sea Res. Part I: Oceanogr. Res. Pap. 51, 1741–1758.

Jones, D.O.B., Bett, B.J., Tyler, P.A., 2007. Megabenthic ecology of the deep Faroe-Shetland channel: a photographic study. Deep-Sea Res. Part I: Oceanogr. Res. Pap. 54 (7), 1111–1128.

Jones, D.O.B., Gates, A.R., Lausen, B., 2012. Recovery of deep-water megafaunal assemblages from hydrocarbon drilling disturbance in the Faroe-Shetland Channel. Mar. Ecol. Prog. Ser. 461, 71–82.

Jones, D.O.B., Mrabure, C.O., Gates, A.R., 2013. Changes in deep-water epibenthic megafaunal assemblages in relation to seabed slope on the Nigerian margin. Deep Sea Res. Part I: Oceanogr. Res. Pap. 78, 49–57.

King, N.J., Bagley, P.M., Priede, I.G., 2006. Depth zonation and latitudinal distribution of deep-sea scavenging demersal fishes of the Mid-Atlantic Ridge, 42 to 53°N. Mar. Ecol. Prog. Ser. 319, 263–274.

Kiriakoulakis, K., Stutt, E., Rowland, S.J., Vangriesheim, A., Lampitt, R.S., Wolff, G.A., 2001. Controls on the organic chemical composition of settling particles in the Northeast Atlantic Ocean. Prog. Oceanogr. 50, 65–87.

Kuhnz, L.A., Ruhl, H.A., Huffard, C.L., Smith Jr, K.L., 2014. Rapid changes and long-term cycles in the benthic megafaunal community observed over 24 years in the abyssal northeast Pacific. Prog. Oceanogr. 124, 1–11.

Lampitt, R.S., 1985. Evidence for the seasonal deposition of detritus to the deep-sea floor and its subsequent resuspension. Deep-Sea Res. 32 (8), 885–897.

Lampitt, R.S., Raine, R.C., Billett, D.S.M., Rice, A.L., 1995. Material supply to the European continental slope: a budget based on benthic oxygen demand and organic supply. Deep-Sea Res. 42 (11–12) (1875-1873).

Lauerman, L.M.L., Kaufmann, R.S., 1998. Deep-sea epibenthic echinoderms and a temporally varying food supply: results from a one year time series in the N.E. Pacific. Deep-Sea Res. Part II: Top. Stud. Oceanogr. 45, 817–842.

Lebrato, M., Jones, D.O.B., 2009. Mass deposition event of *Pyrosoma atlanticum* carcasses off Ivory coast (West Africa). Limnol. Oceanogr. 54 (4), 1197–1209.

Letessier, T.B., Falkenhaug, T., Debes, H., Bergstad, O.A., Brierley, A.S., 2011. Abundance patterns and species assemblages of euphausiids associated with the Mid-Atlantic Ridge, North Atlantic. J. Plankton Res. 33 (10), 1510–1525.

Letessier, T.B., Pond, D.W., McGill, R.A.R., Reid, W.D.K., Brierley, A.S., 2012. Trophic interaction of invertebrate zooplankton on either side of the Charlie Gibbs Fracture Zone/Subpolar Front of the Mid-Atlantic Ridge. J. Mar. Syst. 94, 174–184.

Levin, L.A., 1994. Paleoecology and ecology of xenophyophores. Palaios 9 (1), 32–41.

Levin, L.A., Dayton, P.K., 2009. Ecological theory and continental margins: where shallow meets deep. Trends Ecol. Evol. 24 (11), 606–617.

Levin, L.A., Etter, R.J., Rex, M.A., Gooday, A.J., Smith, C.R., Pineda, J., Stuart, C.T., Hessler, R.R., Pawson, D.L., 2001. Environmental influences on regional deep-sea species diversity. Annu. Rev. Ecol. Syst. 32, 51–93.

Linley, T., Alt, C.H.S., Jones, D.O.B., Priede, I.G., 2013. Bathyal demersal fishes of the Charlie-Gibbs fracture zone region (49° -54°N) of the Mid-Atlantic Ridge: III. Results from remotely operated vehicle (ROV) video transects. Deep-Sea Res. Part II: Top. Stud. Oceanogr. 98, 407–411.

Longhurst, A., 2007. Ecological Geography of the Sea, 2nd edition. Elsevier, London.

Lutz, M.J., Caldeira, K., Dunbar, R.B., Behrenfeld, M.J., 2007. Seasonal rhythms of net primary production and particulate organic carbon flux to depth describe the efficiency of biological pump in the global ocean. J. Geophys. Res. 112 (C10), C10011.

MacArthur, R.H., Wilson, E.O., 1967. The Theory of Island Biogeography. Princeton University Press, Princeton.

McClain, C.R., Barry, J.P., 2010. Habitat heterogeneity, disturbance, and productivity work in concert to regulate biodiversity in deep submarine canyons. Ecology 91 (4).

McClain, C.R., Nekola, J.C., Kuhnz, L., Barry, J.P., 2011. Local-scale faunal turnover on the deep Pacific seafloor. Mar. Ecol. Prog. Ser. 422, 193–200.

Morris, K.J., Bett, B.J., Durden, J.M., Benoist, N.M.A., Huvenne, V.A.I., Jones, D.O.B., Robert, K., Ichino, M.C., Wolff, G.A., Ruhl, H.A., 2016. Landscape-scale spatial heterogeneity in phytodetrital cover and megafauna biomass in the abyss links to modest topographic variation. Sci. Rep. 6, 34080.

Niedzielski, T., Høines, Å., Shields, M.A., Linley, T.D., Priede, I.G., 2013. A multi-scale investigation into seafloor topography of the northern Mid-Atlantic Ridge based on geographic information system analysis. Deep Sea Res. Part II: Top. Stud. Oceanogr. 98 (Part B), 231–243.

Oksanen, J., 2011. Multivariate Analysis of Ecological Communities in R: vegan tutorial.

Palardy, J.E., Witman, J.D., 2011. Water flow drives biodiversity by mediating rarity in marine benthic communities. Ecol. Lett. 14, 63–68.

Priede, I.G., 2009. RRS James Cook JC037. Cruise report, Oceanlab, University of Aberdeen.

Priede, I.G., 2007. RRS James Cook JC011 Cruise report Ecosystem of the Mid-Atlantic Ridge at the Sub-Polar Front and Charlie Gibbs Fracture Zone, 13 July - 18 August 2007, Oceanlab, University of Aberdeen.

Priede, I.G., Bagley, P.M., 2010. RRS James Cook JC048. Cruise report, Oceanlab, University of Aberdeen.

Priede, I.G., Billett, D.S.M., Brierley, A.S., Hoelzel, A.R., Inall, M., Miller, P.I., Cousins, N.J., Fujii, T., 2013a. The ecosystem of the Mid-Atlantic Ridge at the sub-polar front and Charlie-Gibbs Fracture Zone: ECO-MAR project strategy and description of the sampling programme 2007–2010. Deep-Sea Res. Part II: Top. Stud. Oceanogr. 98, 220–230.

Priede, I.G., Bergstad, O.A., Miller, P.I., Vecchione, M., Gebruk, A., Falkenhaug, T., Billett, D.S.M., Craig, J., Dale, A.C., Shields, M.A., Tilstone, G.H., Sutton, T.T., Gooday, A.J., Inall, M.E., Jones, D.O.B., Martinez-Vicente, V., Menezes, G.M., Niedzielski, T., Sigurðsson, Þ, Rothe, N., Rogacheva, A., Alt, C.H.S., Brand, T., Abell, R., Brierley, A.S., Cousins, N.J., Crockard, D., Hoelzel, A.R., Høines, Å., Letessier, T.B., Read, J.F., Shimmield, T., Cox, M.J., Galbraith, J.K., Gordon, J.D.M., Horton, T., Neat, F., Lorance, P., 2013b. Does presence of a Mid-ocean ridge enhance biomass and biodiversity? PLoS One 8 (5), e61550.

R Development Core Team, 2009. R: A language and environment for statistical computing. R Foundation for Statistical Computing. R foundation for Statistical Computing, Vienna, Austria, ISBN 3-900051-07-0.17 URL ⟨http://cran.r-project.org/⟩.

Rex, M.A., 1981. Community structure in the deep-sea benthos. Annu. Rev. Ecol. Syst. 12, 331–353.

Rogacheva, A., Gebruk, A., Alt, C.H.S., 2013. Holothuroidea of the Charlie Gibbs Fracture Zone area, northern Mid-Atlantic Ridge. Mar. Biol. Res. 9, 587–623.

Shields, M.A., Glover, A.G., Wiklund, H., 2013. Polynoid polychaetes of the Mid-Atlantic Ridge and a new holothurian association. Mar. Biol. 9 (5–6), 547–553.

Simon-Lledó, E., Bett, B.J., Huvenne, V.A.I., Schoening, T., Benoist, N.M.A., Jeffreys, R.M., Durden, J.M., Jones, D.O.B., 2019. Megafaunal variation in the abyssal landscape of the Clarion Clipperton Zone. Prog. Oceanogr. 170, 119–133.

Snelgrove, P.V.R., Smith, C.R., 2002. A riot of species in an environmental calm: the paradox of the species-rich deep-sea floor. Oceanogr. Mar. Biol.: Annu. Rev. 40, 311–342.

Soltwedel, T., Jaeckisch, N., Ritter, N., Hasemann, C., Bergmann, M., Klages, M., 2009. Bathymetric patterns of megafaunal assemblages from the arctic deep-sea observatory HAUSGARTEN. Deep-Sea Res. Part I: Oceanogr. Res. Pap. 56, 1856–1872.

Staudigel, H., Hart, S.R., Pile, A., Bailey, B.E., Baker, E.T., Brooke, S., Connelly, D.P., Haucke, L., German, C.R., Hudson, I.R., Jones, D.O.B., Koppers, A.A.P., Konter, J.G., Lee, R., Pietsch, T.W., Tebo, B.M., Templeton, A.S., Zierenberg, R., Young, C.M., 2006. Vailulu'u Seamount, Samoa: life and death on an active submarine volcano. Proc. Natl. Acad. Sci. 103 (17), 6448–6453.

Tilstone, G.H., Miller, P.I., Brewin, R.J.W., Priede, I.G., 2014. Enhancement of primary production in the North Atlantic outside of the spring bloom, identified by remote sensing of ocean colour and temperature. Remote Sens. Environ. 146, 77–86.

Thistle, D., Ertman, S.C., Fauchand, K., 1991. The fauna of the HEBBLE site: patterns in standing stock and sediment-dynamic effects. Mar. Geol. 99 (3–4), 413–422.

Tyler, P.A., Young, C.M., Billett, D.S.M., Giles, L.A., 1992. Pairing behaviour, reproduction and diet in the deep-sea holothurian genus Paroriza (Holothuroidea: Synallactidae). J. Mar. Biol. Assoc. 72, 447–462.

Vecchione, M., Young, R.E., Piatkowski, U., 2010. Cephalopods of the northern Mid-Atlantic ridge. Mar. Biol. Res. 6 (1), 25–52.

Wigham, B.D., Galley, E.A., Smith, C.R., Tyler, P.A., 2008. Inter-annual variability and potential for selectivity in the diets of deep-water Antarctic echinoderms. Deep-Sea Res. Part II: Top. Stud. Oceanogr. 55, 2478–2490.

Wigham, B.D., Hudson, I.R., Billett, D.S.M., Wolff, G.A., 2003. Is long-term change in the abyssal Northeast Atlantic driven by qualitative changes in export flux? Evidence from selective feeding in deep-sea holothurians. Prog. Oceanogr. 59, 409–441.

Wildish, D., Kristmanson, D., 1997. Benthic Suspension Feeders and Flow. Cambridge University Press, Cambridge.

Wolff, G.A., Billett, D.S.M., Bett, B.J., Holtvoeth, J., FitzGeorge-Balfour, T., Fisher, E.H., Cross, I., Shannon, R., Salter, I., Boorman, B., King, N.J., Jamieson, A., Chaillan, F., 2011. The effects of natural iron fertilisation on deep-Sea ecology: the Crozet Plateau, Southern Indian ocean. PLoS One 6 (6), e20697.

Zajac, R.N., 2008. Macrobenthic biodiversity and sea floor landscape structure. J. Exp. Mar. Biol. Ecol. 366, 198–203.